

Isochromat photon map induced by scanning tunneling microscopy from gold particles

T. Umeno and R. Nishitani

Department of Computer Science and Electronics, Kyushu Institute of Technology, Iizuka, Fukuoka 820, Japan

A. Kasuya and Y. Nishina

Institute for Materials Research, Tohoku University, Katahira, Sendai 980-77, Japan

(Received 28 May 1996)

We have measured the maps of isochromat photon intensity induced by scanning tunneling microscopy (STM) from noble metal particles (Au) on a graphite surface. The map is obtained simultaneously with the STM topography image using an optical band-pass filter. The photon map changes depending on the wavelength of the light collected. The isochromat photon maps show that the spectra are varied with the tip position on the particles. This spectra variation is explained by the effect of the change in the tip curvature radius on the spectra of a local plasmon. [S0163-1829(96)02543-X]

I. INTRODUCTION

The photon emission from metal surfaces induced by electron tunneling in scanning tunneling microscopy (STM) is a phenomenon which is related to surface dielectric properties and electromagnetic coupling between the STM tip and the surface. This phenomenon has attracted considerable interest for the surface analysis in a nanometer scale because the intensity map reflects various surface properties in a high resolution of STM.^{1-7,14,15} Some researchers have succeeded in obtaining the STM induced photon maps in ultrahigh vacuum^{3,6,14,15} as well as in air.^{4,5} Berndt *et al.*² and Ito *et al.*⁷ have also measured some spectra for metals. The spectra, however, have been recorded separately from the recording of the STM image. The measurement of spectral resolved photon map has not been made so far.

The photon emission from STM junction is conceived as the radiation from the local plasmon which is excited by inelastic electron tunneling near the local region between the STM tip and the surface of the sample metal.² The nature of the plasmon is determined with the boundary condition of potentials of the STM tip and the metal surface.^{8-10,12} Then the spectra from the local plasmon should be closely related with the geometric structure of the STM tip and the sample metals. In order to study this geometric effect on the STM induced photon spectra as well as the local electronic structure of various materials in a nanometer scale, we need to carry out the spectral mapping of the STM induced light with a simultaneous measurement of an STM image.

In this paper, we report the spectral resolved mapping of STM induced light. The isochromat photon maps show that the spectra are varied with the tip position on the particles. The results indicate the effect of the geometric asymmetry of the STM tip shape on the spectra.

II. EXPERIMENT

A photon mapping measurement is carried out in UHV by a homemade STM combined with a photon detection system. For the STM control and the photon data acquisition, a digital computer system which consists of two microcomputers

and a digital feedback controller is adapted because various and complicated data acquisition is realized by changing the software without a significant change of the hardware.¹¹ We have used a digital signal processor (DSP; TMS320C30, Texas Instrument) for the digital feedback control of the STM.

Photon emitted from the tip-sample junction is collected using an ellipsoidal mirror which is placed such that the tip apex lies at one of its foci, and focused on the second focal point outside the vacuum chamber. Then the focused photon is guided to a photomultiplier (Hamamatsu, R943-02) through optical fibers.

An isochromat photon map is measured by using an optical band-pass filter with the center of the wavelength of 700 and 650 nm and the bandwidth of 80 nm and 30 nm, respectively. The photon map image with 64×64 pixels is obtained simultaneously with the STM topography image with 256×256 pixels. The gold metal films are prepared on the graphite surface by thermal evaporation in a high vacuum of about 1×10^{-7} Torr, and transferred to a UHV chamber for STM measurements without exposing them to air, and measurements are performed at room temperature. The tunneling tips used in the experiments were made by electrochemically etched tungsten wire.

III. RESULTS AND DISCUSSION

Various photon maps and topography images are obtained from gold particles on the graphite surfaces. The photon count is integrated for 0.1 sec at each point of 64×64 points in the scan region. The time for obtaining a photon image is limited by the time for photon counting, and is about 7 min. The photon intensity was recorded at the sample bias of +2.0 V. The photon intensity ranges from 1000 to 20 000 cps at the tunneling current of 10 nA, depending on the condition of the tip and the sample surface. Photon maps observed have shown a spatial resolution of 1 nm at least.

Figures 1(a)–1(d) show a topography image of Au grains (a) and simultaneously recorded photon maps [(b), (c), (d)] of the corresponding area to a STM image with and without a different optical band-pass filter. Figure 1(b) shows an in-

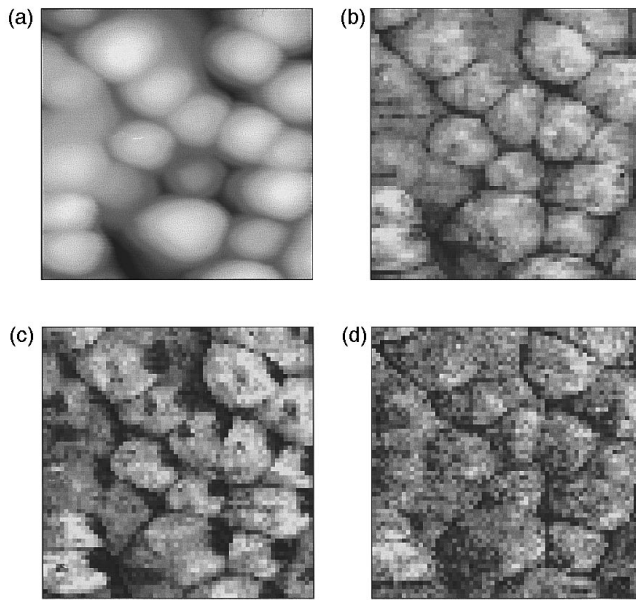


FIG. 1. (a) STM image of gold particles (current 4 nA, sample bias +2 V, scan area $50 \times 50 \text{ nm}^2$). (b) Photon intensity map without an optical filter. (The intensity scale is 20 K cps.) (c) Isochromat photon map with a filter of 700 nm. (The intensity scale is 2 K cps.) (d) Isochromat photon map with a filter of 650 nm. (The intensity scale is 5000 cps.)

egrated photon map without a filter, Fig. 1(c) an isochromat photon map with a filter of 700 nm, and Fig. 1(d) an isochromat map with a filter of 650 nm. The image of Fig. 1(a) is recorded simultaneously with the photon map of Fig. 1(b), so these images have a point to point correspondence between them. The isochromat photon maps of Figs. 1(c) and 1(d), however, are measured in separate scans of the same area as Fig. 1(a) after the integrated photon map [Fig. 1(b)] is recorded, hence a few nanometer drift of the images appear between photon maps.

The nearly spherical Au particles of the size ranging from 10 to 20 nm in diameter are observed both in the STM image and the photon maps. The integrated photon map [Fig. 1(b)] shows a close correlation between the topography and the photon intensity. The detailed comparison between different photon maps [(b)–(d)], however, reveals different correlations between the photon intensity and the topography as follows: As seen in Fig. 1(c), the photon intensity with 700 nm filter is slightly reduced near the center of some grains, and the dark regions are observed on the right side of the grains. In the 650 nm photon map [Fig. 1(d)], on the other hand, the photon intensity tends to increase as it goes from the left to the right sides of the grains. Almost all grains reveal similar asymmetric contrast. In an integrated photon map in Fig. 1(b), such an asymmetry in photon intensity along the grains is not seen, but a symmetric contrast is seen. These results suggest that the location of the tip has an influence on the spectra radiated there. The cross sections of the STM image and the photon map along the line shown in Fig. 1(a) are plotted in Fig. 3(a). These profiles are commonly observed on almost all grains.

On the basis of the above observation, a speculative sketch of the tip location dependent spectra is shown in Fig. 2. If the tip had a symmetric shape, this kind of influence

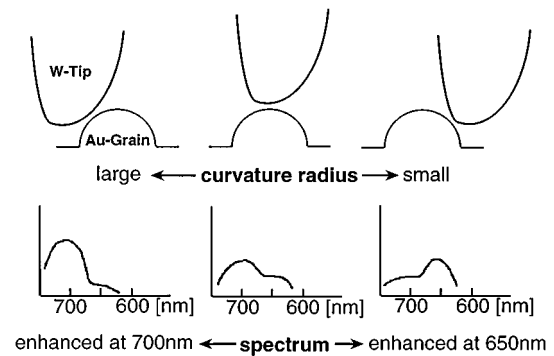


FIG. 2. A speculative sketch of tip location dependent spectra. A redshift with increase in the tip curvature radius is schematically shown.

should not be caused. Then, this phenomenon should be related to the asymmetry of the apex of the STM tip. In fact, as shown in Fig. 3(a), a cross section of the STM image from left to right side of a grain reveals a bilateral asymmetry. It is reasonable to assume that this asymmetry is attributed to a tip shape asymmetry because a bilateral asymmetry of all grains is hardly considered. Based on this fact, if the shape of grains is assumed to be nearly spherical, the tip should have an asymmetric shape as schematically shown in Fig. 3(b). The tip in the present experiment has a larger curvature radius on right side of the tip than left side. The observed change in the contrast of the isochromat photon map in Figs. 1(c) and 1(d) is explained by considering that the larger tip radius causes the increase in intensity of the larger wavelength of the spectra (see Fig. 2). When the tip is located on the right side of the grains, a part of the tip with a smaller tip radius contributes to the plasmon excitation by electron tunneling. Then this situation of plasmon causes a decrease in the intensity of light with the larger wavelength and an increase in that with shorter wavelength, resulting in the observed contrast of photon maps in Fig. 1(c) and Fig. 1(d), respectively. This explanation on the basis of the redshift of spectra due to larger tip radius is consistent with the theoretical prediction of the spectra of the local plasmon, in which the emission spectra is obtained by calculating the power spectrum of the radiation from the effective dipole¹³ produced at the STM junction by the Green function method.¹⁰ In the interpretation of the result, we may consider the effect of the contamination on the STM tip. If the tip is partially coated with gold from the sample then the spectra would be expected to depend on the tip position above the gold particles. This effect, however, can be distinguished from the tip-radius effect in the above observation since the gold on the tip causes a more drastic change in the spectra than the tip-radius effect based on the calculation of the emission spectra as described in the next paragraph. This effect may be found in the dark region in Fig. 1(c). Therefore, the present study presents an experimental observation of the tip-radius effect on the spectra of the local plasmon in STM junction.

The dark regions on the right side of grains in Fig. 1(c) may be attributed to a different origin. The dark regions are observed only in the 700 nm photon map, indicating a drastic change in the spectrum for the dark regions. This fact sug-

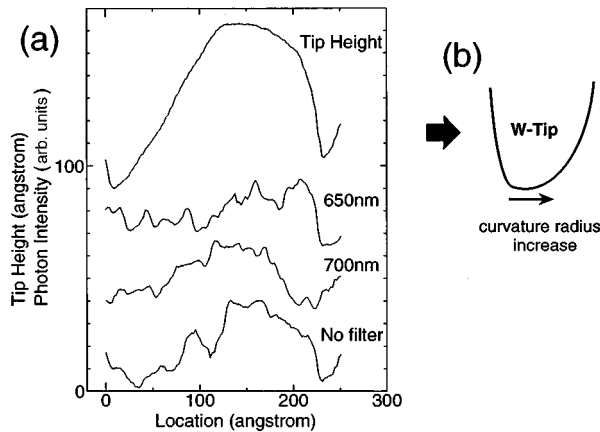


FIG. 3. (a) A cross section of the STM image and the photon maps from the left to the right side of a grain. An asymmetry of the STM image and isochromat photon maps is observed. These profiles are commonly observed on almost all grains. (b) A tip shape speculated from the cross section of the STM image.

gests that the emission in the dark regions has a rather narrow spectral width which is different from the spectra in other regions. Therefore the dark regions may be originated from an impurity on the left side of the tip apex, such as a gold adhesion from the sample. This interpretation is supported by a calculation of an emission spectrum by the method as mentioned above for the tunnel junction of the Au tip and the Au sample. The calculation shows a narrow spec-

trum with the width of about 26 nm in contrast to the broad spectrum for the W tip and the Au sample.

Ito *et al.* have made spectral measurements at different tip positions on the Au grain,⁷ and they have reported that a spectral mode with a shorter wavelength is enhanced at the grain edge. They suggest that the enhancement of this mode at the grain edge is attributed to the excitation of a multipole mode of the plasmon. Their discussion is based only on the geometry of the sample. The present results, however, have suggested that the spectral mode of STM induced light depends not only on the sample geometry but also the tip geometry. In order to clarify further the mechanism of light emission in STM, a two-dimensional mapping of the spectra is in progress.

IV. CONCLUSION

In conclusion, maps of isochromat photon intensity induced by STM are obtained simultaneously with the topography image. The detailed comparison between the isochromat photon maps and the topography shows that the variation in contrast of the photon map is influenced by the tip geometry which induces the change in the spectra: a redshift of the spectrum with increase in a tip radius. This result is in a qualitative agreement with a theoretical prediction.

ACKNOWLEDGMENTS

This work is supported in part by a Grant-in-Aid from the Ministry of Education, Science and Culture, and Research Foundation For Materials Science.

- ¹J.K. Gimzewski, B. Reihl, J.H. Coombs, and R.R. Schlittler, *Z. Phys. B* **72**, 497 (1988).
- ²R. Berndt, J.K. Gimzewski, and P. Johansson, *Phys. Rev. Lett.* **67**, 3796 (1991).
- ³R. Berndt and J. Gimzewski, *Phys. Rev. B* **48**, 4746 (1993).
- ⁴N. Venkateswaran, K. Sattler, J. Xhie, and M. Ge, *Surf. Sci.* **274**, 199 (1992).
- ⁵V. Sivel, R. Coratger, F. Ajustron, and J. Beauvillain, *Phys. Rev. B* **45**, 8634 (1992).
- ⁶A.W. McKinnon, M.E. Welland, T.M.H. Wong, and J. K. Gimzewski, *Phys. Rev. B* **48**, 15 250 (1993).
- ⁷K. Ito, S. Ohyama, Y. Uehara, and S. Ushioda, *Surf. Sci.* **324**, 282 (1995).
- ⁸P. Johansson, R. Monreal, and P. Apell, *Phys. Rev. B* **42**, 9210 (1990).
- ⁹B.N.J. Persson and A. Baratoff, *Phys. Rev. Lett.* **68**, 3224 (1992).
- ¹⁰Y. Uehara, Y. Kimura, S. Ushioda, and K. Takeuchi, *Jpn. J. Appl. Phys.* **31**, 2465 (1992).
- ¹¹R. Nishitani, K. Suga, and T. Miyasato, *Abstract of 40th International Field Emission Symposium, Nagoya, Japan* (International Field Emission Society, Nagoya, 1993), p. 144.
- ¹²P. Johansson and R. Monreal, *Z. Phys. B* **84**, 269 (1991).
- ¹³R.W. Rendell and D.J. Scalapino, *Phys. Rev. B* **24**, 3276 (1981).
- ¹⁴R. Berndt, R. Gaisch, W.D. Schneider, J.K. Gimzewski, B. Reihl, R.R. Schlittler, and M. Tschudy, *Appl. Phys. A* **57**, 513 (1993).
- ¹⁵R. Berndt, R. Gaisch, W.D. Schneider, J.K. Gimzewski, B. Reihl, R.R. Schlittler, and M. Tschudy, *Phys. Rev. Lett.* **74**, 102 (1995).